Organic Electronics 13 (2012) 252–263

Contents lists available at SciVerse ScienceDirect

Organic Electronics

journal homepage: www.elsevier.com/locate/orgel

Photovoltaic properties of low band gap copolymers based on phenylenevinylene donor and cyanovinylene 4-nitrophenyl acceptor units

G.D. Sharma [b,c,*], J.A. Mikroyannidis [a], Surya Prakash Singh [d]

[a] Chemical Technology Laboratory, Department of Chemistry, University of Patras, GR-26500 Patras, Greece
[b] Physics Department, Molecular Electronic and Optoelectronic Device Laboratory, JNV University, Jodhpur, Rajasthan 342005, India
[c] R&D Center for Science and Engineering, Jaipur Engineering College, Kukas, Jaipur, Rajasthan, India
[d] Inorganic and Physical Chemistry Division, Indian Institute of Chemical Technology, Hyderabad 500607, India

ARTICLE INFO

Article history:
Received 5 July 2011
Received in revised form 3 October 2011
Accepted 23 October 2011
Available online 26 November 2011

Keywords:
Phenylenevinylene copolymer
Cyanovinylene 4-nitrophenyl
Low band gap
Bulk heterojunction solar cells
Modified PCBM i.e. **F**

ABSTRACT

Two novel copolymers **P1** and **P2** having phenylenevinylene donor and cyanovinylene 4-nitrophenyl acceptor units, were synthesized by heck coupling and employed as electron donor along with PCBM or modified PCBM (**F**) as electron acceptor for the fabrication of bulk heterojunction (BHJ) photovoltaic devices. These copolymers **P1** and **P2** showed broad band absorption around 640–700 nm and optical band gap of 1.60 eV and 1.72 eV, respectively. The highest occupied molecular orbital (HOMO) and lowest unoccupied molecular orbital (LUMO) estimated from cyclic voltammetry measurement reveals that these values are well suitable for the use of these copolymers as electron donor along with PCBM derivatives as electron acceptor for BHJ active layer. The suitable LUMO off set allows efficient photo-induced charge transfer at the donor/acceptor interfaces in the BHJ photovoltaic device and resulting power conversion efficiency (PCE) of 2.8% and 3.29% for **P1** and **P2**, respectively, when PCBM is used as acceptor. This value has been improved up to 3.52% and 4.36% for the devices based on **P1** and **P2** when **F** is used as electron acceptor, instead of PCBM. We have also investigated the effect of solvent annealing on the photovoltaic performance of device based on **P1**: F and **P2**: F blends and found that the over all PCE of the devices is 4.36% and 4.88%, respectively. The increase in PCE is mainly due to the improvement in the J_{sc}, which is due to the increased charge transport in the annealed device as compared to as cast device.

1. Introduction

Organic π-conjugated polymers and small molecules constitute an important class of functional materials [1]. Their abilities to act as semiconductors and to facilitate charge transport had led to their use as the active materials in various optoelectronics devices such as light emitting diodes (LEDs) and solar cells [2]. In recent years, polymer solar cells (PSCs) have attracted considerable attention because of their advantages of low cost, easy to fabrication, light weight, and the capability to fabricate flexible large area devices [3]. Solar cells based on organic semiconductor donor/acceptor (D/A) interfaces have the potential to provide a cost effective alternative photovoltaic technology for power generation. The highest performing organic semiconductor devices employ a bulk heterojunction (BHJ) architecture containing highly intermixed blends of conjugated polymer donors and fullerene derivative acceptors [4]. One of the most critical processes in organic photovoltaic devices is free charge carrier generation from the photogenerated excitons, at the D/A interfaces [5].

* Corresponding author at: Physics Department, Molecular Electronic and Optoelectronic Device Laboratory, JNV University, Jodhpur (Rajasthan) 342005, India.
E-mail address: sharmagd_in@yahoo.com (G.D. Sharma).

1566-1199/$ - see front matter © 2011 Elsevier B.V. All rights reserved.
doi:10.1016/j.orgel.2011.10.022

Generally, a high efficient photovoltaic device needs both a photoactive layer with excellent light absorption capabilities and large D/A interfacial area for efficient dissociation of photogenerated excitons into free electrons and holes. Therefore, the lowest unoccupied molecular orbital (LUMO) offset between the donor polymer and fullerene acceptor must be larger enough (normally in the range 0.3–0.4 eV) to ensure the efficient dissociation of excitons [3g]. Power conversion efficiencies (PCEs) approaching 5% have been realized using poly (3-hexylthiophene) (P3HT) and fullerene derivatives as electron donor and electron acceptor, respectively in BHJ active layer [6]. Recently, Li et al. have used different types of new fullerene derivatives as electron donor for the BHJ polymer solar cells and achieved a PCE more than 6% for polymer solar cell with a blend of P3HT and new fullerene derivative [7]. However, further improvement in the PCE for BHJ solar cells based on P3HT:PCBM blend is limited by the relatively large band gap of P3HT (1.9 eV), which limits the harvest of solar light beyond wavelength region 620 nm and relatively small energy difference between the LUMO of PCBM and HOMO of P3HT, resulting low value of open circuit voltage (V_{oc}). For an industrial point of view, solar cells should exhibit a PCE of around 10% [8]. The design of new active layer materials with appropriate properties is one of the main approaches toward high performance PSCs. Optical band gap is one of the key parameters of the active layer for PSCs. In order to harvest more sunlight, the mismatch between the absorption spectrum of active materials and solar spectrum should be minimized. The optoelectronic properties of conjugated polymer semiconductors are primarily governed by the conjugated blocks incorporated in the polymer backbone. It has been well proven that the incorporation of electron donating (D) and electron accepting (A) units in the main backbone is one of the most promising and alternative strategies for making low band gap organic semiconducting polymers [3c,9]. Selection of such D–A units in the conjugated backbone requires special attention paid to certain properties such as electron donating or accepting capability and efficient tunability of electronic characteristics through side chain substitution. Such a D–A combination allows for the band gap tuning through hybridization of the HOMO of the donor moiety with LUMO of the acceptor moiety and has been used effectively to lower the band gap of conjugated polymers copolymers and also enhance the charge carrier mobility due to the reduced interchain π–π stacking distance [10]. Through the donor–acceptor intrachain charge transfer (ICT) method, as series of low band gap polymers have been synthesized in recent years on D–A copolymerization and shown efficient photovoltaic response [11]. The power conversion efficiency (PCE) of the BHJ polymer solar cells based on D–A copolymers has steadily increased in recent years and reached in the range 6–7.4% [12]. To date the PCEs based on conjugated copolymers polymer solar cells have reached as high up to 8.13% and 8.3% by Solarmer [13a] and Konarka [13b], respectively. These advances in solar cells has came largely through the synthesis of new materials having a modified electronic structure to optimally harvest the sun light (materials with a small bandgap) and ability to separate the excitons into free charge carriers.

Various low band gap small molecules and polymers carrying cyanovinylene 4-nitrophenyls have been synthesized by Mikroyannidis et al., and used for BHJ solar cells [14] and dye-sensitized solar cells [15] with enhanced efficiency. Recently, Mikroyannidis and Sharma have synthesized two low band gap phenylenevinylene copolymers with cyanovinylene 4-nitrophenyl segments and used as electron donor for BHJ solar cells reported PCE of 4.0% [16]. The present investigation deals with the optical and electrochemical properties of the two low band gap D–A copolymers **P1** and **P2**. In these copolymers cyanovinylene 4-nitrophenyl group behave as electron acceptor and phenylenevinylene unit as electron donor. We have fabricated the BHJ photovoltaic devices employing blend photoactive layer in which these copolymers are used as electron donor and PCBM and modified PCBM (**F**) as electron acceptor. We have achieved a PCE of 2.8% and 3.29% for **P1** and **P2**, respectively, when PCBM is used as acceptor. The PCE value has been improved up to 3.72% and 4.36% for the devices based on **P1** and **P2** when modified **F** [17] is used as electron acceptor, instead of PCBM. The PCE value of **P1**:**F** and **P2**:**F** has been further improved up to 3.68% and 4.6%, respectively, when the BHJ layer is solvent annealed. The higher value of PCE for the device based on solvent annealed active layer has been attributed to the more balanced charge transport in the device due to the increased hole mobility.

2. Experimental part

All the chemicals were purchased from Sigma–Aldrich used without further purification. The copolymers poly [[2,5-bis [2-cyano-2-(4-nitrophenyl) ethenyl]-1,4-phenylene]-1,2-ethenediyl [2,5-bis (hexyloxy)-1,4-phenylene]-1,2-ethenediyl] (**P1**) and poly[[(4-formylphenyl)imino]-1,4-phenylene-1,2-ethenediyl [2,5-bis(hexyloxy)-1,4-phenylene]-1,2-ethenediyl-1,4-phenylene] (**P2**) were synthesized with the similar procedure as reported earlier [16] and the chemical structure of the conjugated polymers **P1** and **P2** are shown in Chart 1. The synthesis of modified PCBM i.e. 3′H-Cyclopropa[1,9][5,6]fullerene-C60-Ih-3′-butanoic acid, 3′-phenyl-, 4-[2-cyano-2-(4-nitrophenyl) ethenyl]phenyl ester (**F**) was already reported earlier [17]. Organic photovoltaic (OPV) devices were fabricated on indium tin oxide (ITO) coated glass substrates with a configuration ITO/PEDOT:PSS/polymers: PCBM derivatives blend/Al. The ITO coated glass substrates were cleaned by ultrasonication sequentially in detergent, water, acetone and 2-propanol and then dried overnight in oven. A layer of PEDOT:PSS (~60 nm) was spin coated on the substrate at 1500 rpm using an aqueous solution of PEDOT:PSS (Baytron) and then dried for 10 min at 100 °C. The BHJ active layer (**P1** or **P2**:PCBM derivative acceptors i.e. PCBM and **F** chemical structure shown in Chart 1) was then deposited by spin coating a solution of (10 mg/mL) of polymer (50 wt.%) and PCBM derivative (50 wt%) in a THF solvent, at rpm 2500 rpm on the top of PEDOT:PSS layer and then

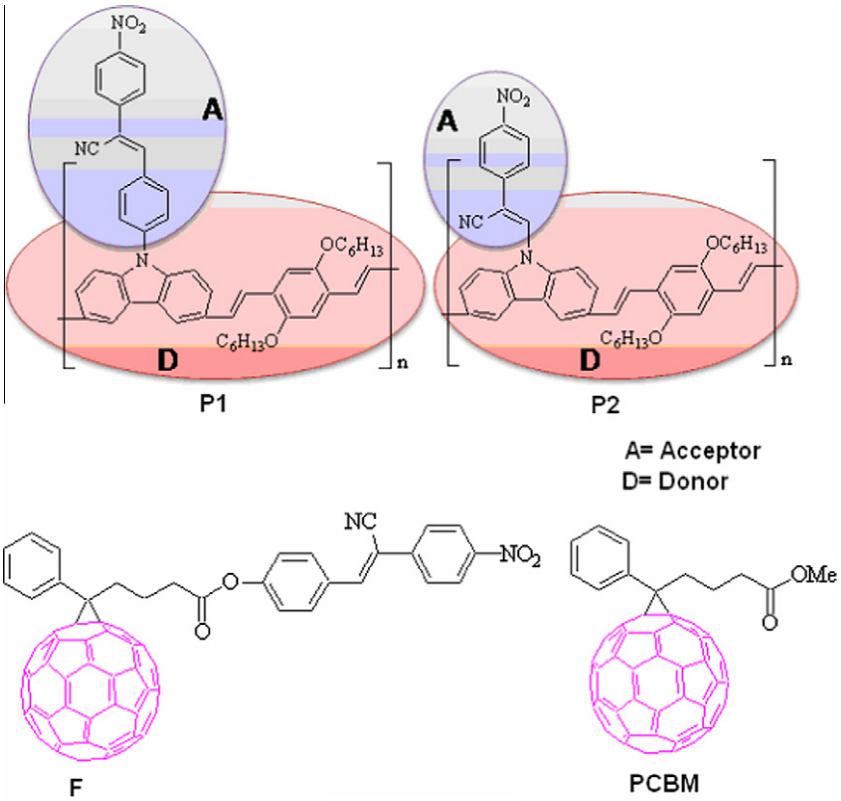

Chart 1. Chemical Structure of **P1**, **P2**, PCBM and **F**.

dried at room temperature for 1 h to remove the excess solvent. The film thickness of BHJ active layer was optimized by changing the spinning speed during the spin coating. The thickness of the BHJ active layer used in the OPV devices is around 90 nm. An aluminum (Al) cathode was deposited by thermal evaporation through a shadow mask (area 5 mm^2) under a pressure of $\sim 10^{-5}$ Torr to complete the device.

The solvent annealing treatment of the polymer:PCBM blend films were carried out before the deposition of the metal electrode. The samples were transferred into a glass jar filled with DCB, where they remained for 30 min. The solvent annealing was controlled by the slow evaporation rate of the solvent, which was carried out by adding a small amount of solvent into the glass jar to keep the film wet until it had completely solidified.

Current density–voltage (J–V) characteristics (in dark and under illumination) of the devices were measured using a Keithley 238 source meter unit. The measurements were conducted in air under the irradiation of AM 1.5 simulated solar light (100 mW/cm^2). Light intensity was adjusted by using a standard luxmeter with an optical filter.

The hole-only devices ITO/PEDOT: PSS/**P2**:**F**/Au, were used to estimate the hole mobility in the blend films and were fabricated as described above except that the top electrode was replaced with Au. Electron-only devices having structure Al/**P2**:**F**/Al was also fabricated by spin-coating the active layer on glass/Al substrates, followed by deposition of the Al electrode.

3. Results and discussion

3.1. Optical and electrochemical properties

The absorption spectra of both the polymers in THF solution and thin films are shown in Fig. 1a and b, respectively. The absorption spectra in thin film have normalized with respect to longer wavelength peak. Both the polymers showed two absorption peaks, which is a common feature of donor–acceptor type copolymers [17]. In the polymer solution, the maximum absorptions of the copolymers at 390 nm for **P1** and 396 nm for **P2** corresponds to the π–π^* transition of the polymer backbone. The absorption peak at longer wavelength region corresponds to the intramolecular charge transfer (ICT) from the donor to the acceptor in the copolymers. When the maximum absorption wavelengths of the polymers in solution are compared with those in thin film, it reveals that both the polymers show a pronounced peak broadening and red shift of absorption edges, indicating that the polymer chains are highly aggregated in the solid state. The optical bandgaps (E_g^{opt}), as determined from the onset of the absorption spectra of the polymers are 1.72 eV and 1.60 eV for **P1** and **P2**,

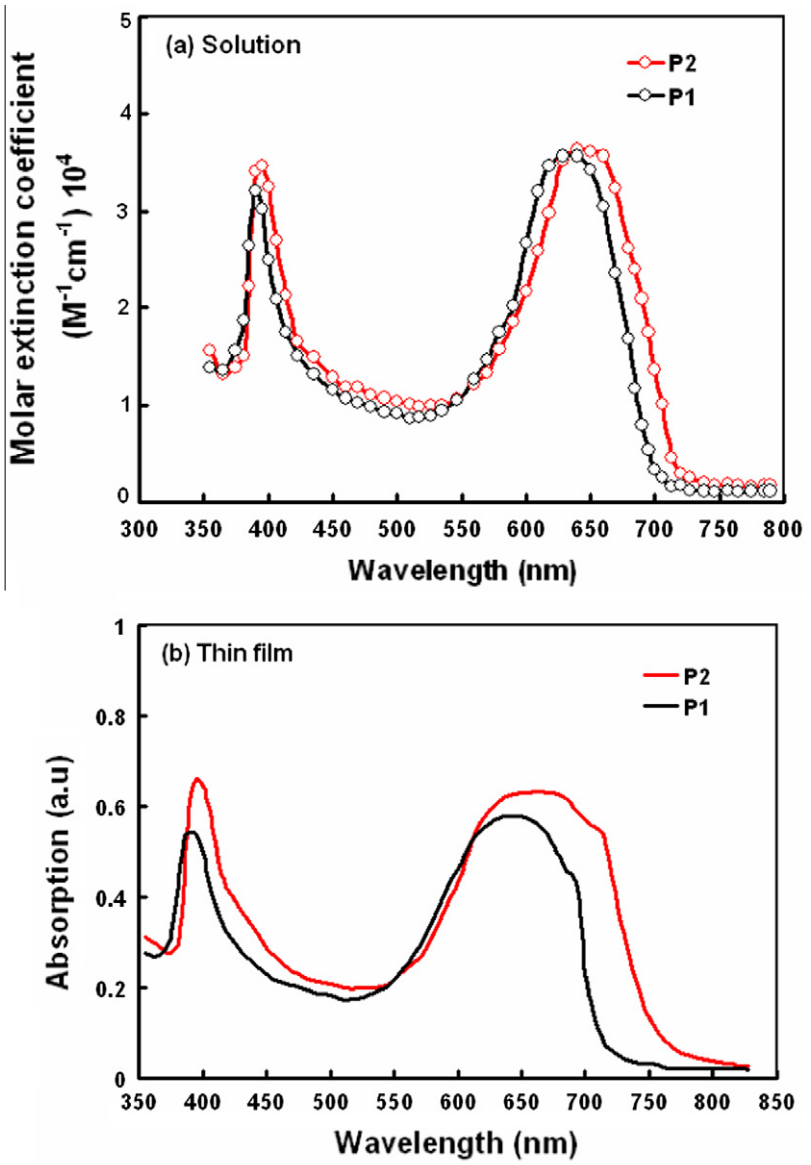

Fig. 1. UV–visible absorption spectra of **P1** and **P2** in (a) THF solution and (b) thin films cast from THF solvent.

respectively. These values are close to the ideal bandgap (1.5–1.7 eV) of polymer solar cells [8]. The value of optical band gap is comparable with other related organic materials as reported earlier [14a,18] and much smaller than most commonly used conjugated polymer P3HT (1.90 eV).

The electrochemical data of polymers are obtained from the oxidation and reduction cyclic voltammograms, as shown in Fig. 2. It can be seen from these curves that both the polymers exhibit reversible cathodic reduction and anodic oxidation curves in cyclic voltammetry measurements. Based on the onset potentials of oxidation (E_{ox}^{onset}) and reduction ((E_{red}^{onset}) processes, the HOMO) and LUMO energy levels of the polymers are estimated from the following expression [19]

$$\text{HOMO} = -(E_{ox}^{red} + 4.70)\ \text{eV}$$

$$\text{LUMO} = -(E_{red}^{onset} + 4.70)\ \text{eV}$$

The HOMO and LUMO energy levels of polymers are estimated from the onset oxidation and reduction potentials, assuming the absolute redox potential of reference Ag/Ag+ electrode to be 4.7 eV below vacuum. The HOMO energy levels of the polymers, estimated from above equation, are −5.26 eV and −5.2 eV, for **P1** and **P2**, respectively. The LUMO levels of the **P1** and **P2**, calculated from the onset reduction potentials are – 3.40 eV and −3.44 eV for **P1** and **P2**, respectively. It has been reported that the threshold HOMO level for the air stable conjugated polymers being estimated to be −5.2 eV [20], the lower HOMO level

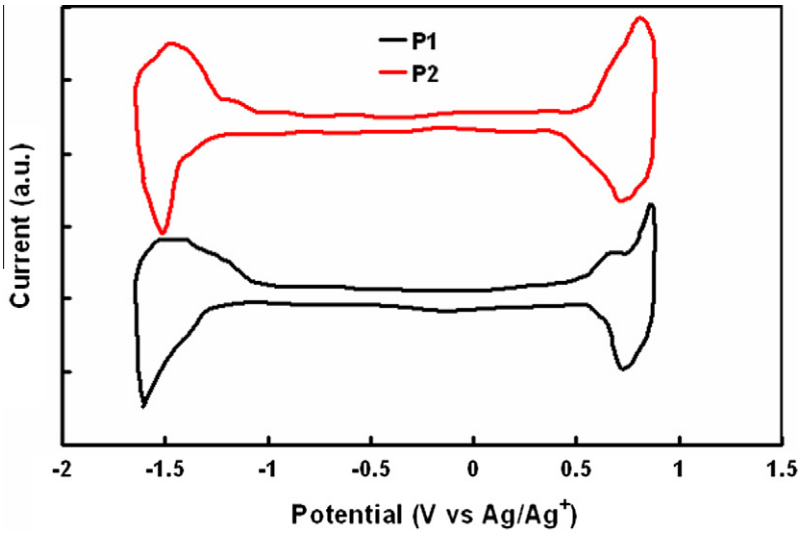

Fig. 2. Cyclic voltammetry of **P1** and **P2** in $TBAPF_6$ (0.1 M) at scan rate 100 mV/s using carbon glassy rod, Ag/AgCl and Pt wire as working, reference and counter electrodes, respectively.

of these two polymers should be beneficial to their chemical stability. Since the open circuit voltage (V_{oc}) of polymer solar cells is linearly dependent on the difference between the HOMO level of the electron donor and the LUMO level of the electron acceptor, used in the BHJ active layer, the low-lying HOMO level of the donor polymer is expected to afford a high V_{oc} for resulting polymer solar cells. Moreover, considering that a LUMO–LUMO offset of 0.3–0.4 eV [21] is necessary for efficient electron transfer from donor polymer to fullerene derivative, is expected that the excitons can be easily dissociated at the interface between the these polymers and fullerene derivates, because the LUMO levels of polymer (−3.40 to −3.44 eV) are sufficiently higher than that of fullerene derivatives (−4.0 eV to −3.75 eV). Therefore, from these electrochemical characteristics, it is concluded that these two polymers are promising electron donor materials along with fullerene derivatives for BHJ polymer solar cells.

3.2. Electrical properties of polymers

We have investigated the J–V characteristics of **P1** and **P2** using a single layer device having structure ITO/PEDOT:PSS/**P1** or **P2**/Al in dark as shown in Fig. 3a. The J–V characteristics of the device in the dark show a rectification effect when positive potential is applied to the ITO/PEDOT:PSS electrode with respect to the Al electrode. Since the HOMO level of **P1** (−5.26 eV) or **P2** (5.2 eV) is very close to the work function of PEDOT:PSS (−5.1 eV), the PEDOT:PSS/**P1** or **P2** interface behaves as Ohmic contact in their respective devices, for hole injection from the PEDOT:PSS into the HOMO level of polymer. However, the LUMO level of these polymers (−3.40 and 3.44 eV) is very far from the work function of Al (−4.2 eV), the polymer–Al interface behaves as Schottky barrier for the electron injection from the Al into the LUMO level of Polymer. Therefore, the rectification observed in the J–V characteristics in dark is due to the formation of a Schottky barrier at the Al/polymer interface and both the polymers behaves as p type organic semiconductor and can be used as electron donor component along with PCBM as electron acceptor for BHJ active layer.

Charge carrier mobility in the conjugated polymer is important to the performance of the BHJ polymer solar cells. We have estimated the hole mobility in the polymers measuring the current–voltage characteristics in dark for nearly hole only devices. We have fabricated nearly hole only device having structure ITO/PEDOT:PSS/**P1** or **P2**/Au device. Since the work function of Au is about 4.8 eV, we assume that Au form a nearly ohmic contact with the both polymers. In these devices both interfaces behaves as ohmic contact.

The hole mobilities of an organic semiconductor can be estimated from the J–V characteristics in the dark using space charge limited current (SCLC) with trap free limit. The current in this limit can be expressed as [22]

$$J_{SCLC} = (9/8)\varepsilon_0\varepsilon_r\mu_h(V^2/d^3) \quad (1)$$

where J_{SCLC} is the current density in SCLC region, ε_o is the permittivity of free space, ε_r is the dielectric constant of the material, μ_h is the hole mobility, V is the applied voltage corrected for built in voltage (V_{bi}) arising from the work function of the electrodes, and d is the thickness of the organic layer. We have investigated the J–V characteristics of the device having structure ITO/PEDOT:PSS/**P1** or **P2**/Au and shown in Fig. 3b. It can be seen from this figure that in the higher voltage region above 0.48 V, the current can be fitted with the Eq. (2). The hole mobilities estimated from intercepts of corresponding lines in SCLC region are 1.65×10^{-4} and 7.4×10^{-5} cm^2/Vs for **P2** and **P1,** respectively.

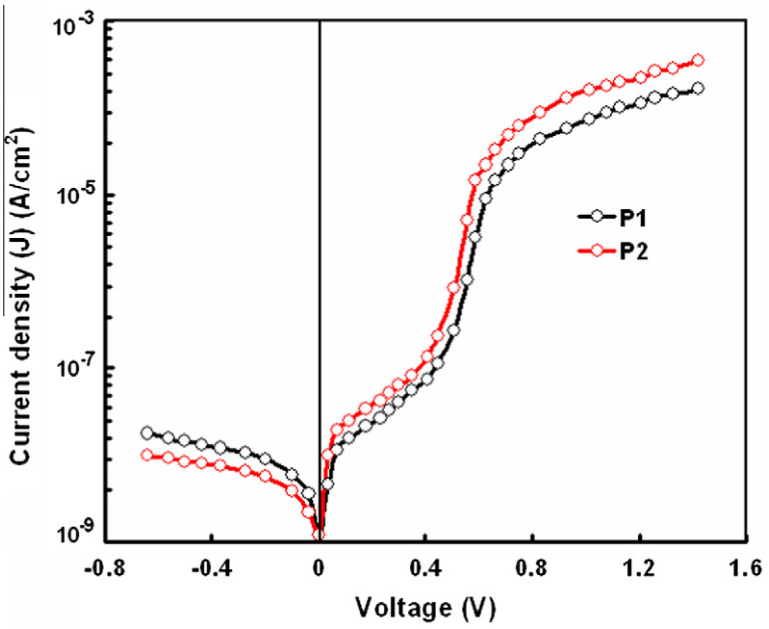

Fig. 3a. Current–voltage (J–V) characteristics of ITO/PEDOT:PSS/**P1** or **P2**/Al devices, in dark

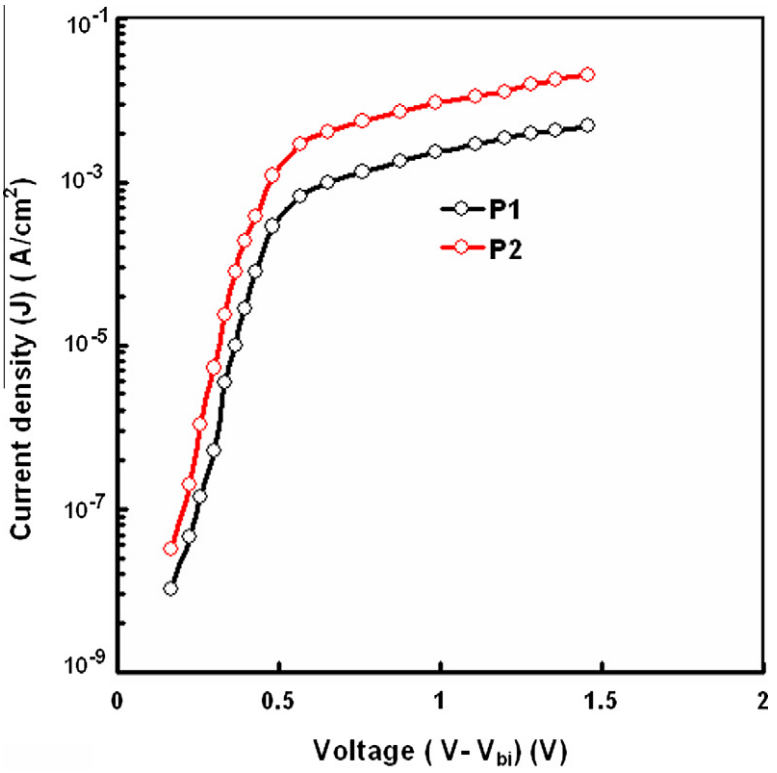

Fig. 3b. Current–voltage characteristics of ITO/PEDOT:PSS/**P1** or **P2**/Au devices for the estimation of hole mobility.

3.3. Photovoltaic properties of BHJ devices

The photovoltaic properties of the polymers were investigated with a conventional device configuration of ITO/PEDOT:PSS/polymer: PCBM or modified PCBM i.e. **F**/Al. The weight ratio of donor and acceptor is 1:1. Fig. 4a and b show the current–voltage (J–V) characteristics of the devices based on **P1** and **P2** as electron donor and PCBM and

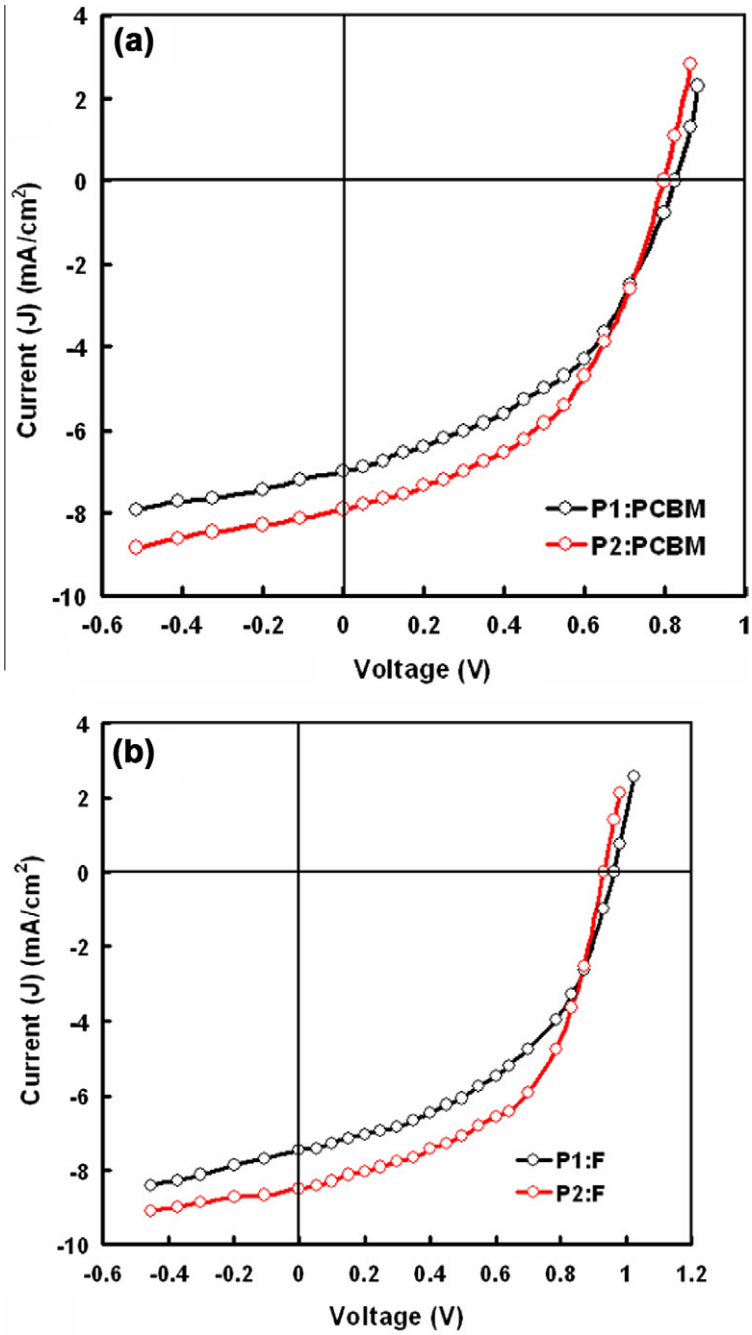

Fig. 4. Current–voltage characteristics, under illumination of the BHJ devices based on (a) **P1**:PCBM and **P2**:PCBM and (a) **P1**:**F** and **P2**:**F** blends.

F as electron acceptor and photovoltaic parameters are complied in Table 1. The device based on **P1**:PCBM shows a open circuit voltage V_{oc} of 0.83 V, a short circuit current J_{sc} of 7.0 mA/cm^2, and a fill factor of 0.48, resulting PCE if 2.8%. However, the device based on **P1**:**F** shows V_{oc} of 0.96 V, J_{sc} of 7. 46 mA/cm^2 and a fill factor of 0.52, resulting a PCE of 3.72%. Under the same conditions, the **P2**:PCBM device showed a PCE of 3.29% with a V_{oc} of 0.80 V, J_{sc} of 7.9 mA/cm^2 and FF of 0.52. The device based on **P2**:**F** showed a PCE of 4.36% with V_{oc} of 0.93, J_{sc} of 8.52 mA/cm^2 and FF of 0.55. The values of both J_{sc} and FF for the device based on **P2**:**F** are higher than that for **P2**:PCBM, resulting improved value of over all PCE. The J_{sc} mainly depends on the number of excitons generated in the photoactive layer after the absorption of light, and their dissociation into free charge carriers at D–A interfaces present in the BHJ active layer and their transportation towards the collecting electrodes. The number of excitons

Table 1
Photovoltaic parameters of BHJ solar cells using different blends.

Blend	J_{sc} (mA/cm^2)	V_{oc} (V)	FF	PCE (%)
P1:PCBM	7.0	0.83	0.48	2.8
P1:**F**	7.46	0.96	0.52	3.72
P2:PCBM	7.9	0.80	0.52	3.29
P2:**F**	8.52	0.93	0.55	4.36
P1:**F**[a]	8.6	0.94	0.54	4.36
P2:**F**[a]	9.69	0.90	0.56	4.88

[a] Solvent anealing.

generated in the active layer mainly depends on the band gap and optical absorption spectra of the material used as photoactive layer in the device. Lower band gap and broader absorption spectra in longer wavelength region, of **P2** as compared to **P1** imply that number of excitons generated in the photoactive layer with **P2** is higher than that for the photoactive layer with **P1**. Moreover, the higher value of hole mobility in the **P2** results more efficient charge transfer in the device based on **P2**. We conclude that the higher light harvesting property of the blend based on **P2** leads to higher exciton generation in the photoactive layer, resulting higher photocurrent in the device.

The over all PCE of the BHJ photovoltaic devices based on **F** as electron acceptor is higher than that for the devices based on PCBM as electron acceptor, which is attributed to the increase in both J_{sc} and V_{oc}. Since, in the BHJ photovoltaic device, the V_{oc} is directly related to the energy difference in the LUMO of electron acceptor and HOMO of donor employed in the photoactive layer. The LUMO of the **F** is about −3.75 eV, which is higher than that of PCBM (−4.0 eV). The higher value of LUMO for **F** is attributed to the higher value of V_{oc} for the devices based on **F** electron acceptor. The value of J_{sc} is related with the light absorption capabilities of the photoactive layer and number of the exciton generated in photoactive layer after the absorption of light. We have already reported that the **F** shows stronger absorption in the wavelength region 300–550 nm in comparison to PCBM [17], therefore the light harvesting capability has been improved for the blend of polymer (**P1** or **P2**) with **F** in this wavelength region, which is missing for the blend based on PCBM. We conclude that the increase in the J_{sc} for the devices based on **F** as electron acceptor is due to the improved light harvesting property of blend and generation of more excitons, resulting more free charge carriers.

The over all PCE of the devices based on these copolymers is still low for the commercial applications. It has been reported that photocurrent generation in the BHJ photovoltaic device is determined by the three processes: the diffusion of exciton towards the D/A interface, exciton dissociation into free charge carriers and the collection of charge carriers by the electrodes [23]. The diffusion of the excitons towards the D/A interface in the BHJ photoactive depends on the nanoscale morphology of the blend. The charge carrier transport depends upon the separate interpenetrating percolated paths for electron and hole towards the collecting electrodes.

We have investigated the effect of solvent treatment (annealing) of BHJ active layer on the photovoltaic response of the BHJ devices based on **P1**:**F** and **P2**:**F** blends. The J–V characteristics of the devices under the illumination intensity of 100 mW/cm^2 are shown in Fig. 5 and the photovoltaic parameters are complied in Table 1. The overall PCE of the devices based on solvent annealing **P1**:**F** and **P2**:**F** are 4.36% and 4.88%, respectively. The increase in the PCE for the device based on solvent annealed photoactive layer is mainly due to the increase in the J_{sc} and FF as compared to the device based on as cast active layer. However, there is a slight decrease in the V_{oc}, which is compensated by the increase in both J_{sc} and FF. The increase in the PCE of the device upon solvent annealing can be understood in terms of improvement in the light absorption, by extending the conjugation length and balance charge transport, by increasing the hole mobility of the conjugated copolymer. These results were mainly attributed to the improved morphology of the copolymer, which can easily self organize into well ordered chain during the solidification through the solvent annealing.

The information about the degree of crystallinity in the copolymer film can be evaluated by investigating the optical absorption spectra of the blends (as cast and solvent annealed blend). We have recorded the optical absorption spectra of the **P1**:**F** and **P2**:**F** blends (as cast and treated with DCB for 10 min) and shown in Fig. 6 for **P2**:**F** blend. Similar results have been also observed for **P1**:F blend. It is found that the broad absorption band, red shift in the absorption peak and enhanced absorption intensity and clearly observed vibronic shoulder in longer wavelength region for solvent annealed **P2**:**F** film is attributed to the enhanced conjugation length and more ordered structure of the copolymer. During the solvent annealing process, the solvent molecules penetrate into the film and increase the space between copolymer chains and the chains become more mobile and self organization occurs to form the ordering.

Thin film XRD was used to get information about the difference in the crystallinity of the copolymer: **F** blended films (as cast and solvent annealed). The XRD patterns of the **P2** (as cast), **P2**:F (as cast) and **P2**:**F** (solvent annealed) are shown in Fig. 7. It can be seen from this figure that the pristine as cast **P2** film exhibits a sharp XRD band with a peak centered at $2\theta = 7.75°$, which is related to the interplanar distance of 9.6 A°. When the **P2** is blended with the **F**, this peak become weak and is broadened suggesting effective mixing of **F** with **P2**. However, when the **P2**:F blend is solvent annealed, this peak again reappears. This indicates that blend film cast from the THF solvent was not sufficiently crystallized. However, when the film cast from THF solvent is treated with DCB, the crystallinity of the blend is increased. The change in the film crystallinity with the solvent annealing agrees with the change observed in the absorption spectra. Since most of the fullerene derivatives do not show any diffraction peak in the range 2θ values (4–10°) [24], we assume that the change in the crystallinity after solvent annealing is mainly attributed to the increased crystallinity of copolymer **P2**.

In BHJ photovoltaic devices the ratio of electron and hole mobilities plays an important role in deciding the charge collection efficiency and therefore the PCE of the device. The hole and electron mobilities of **P2**:**F** blend film

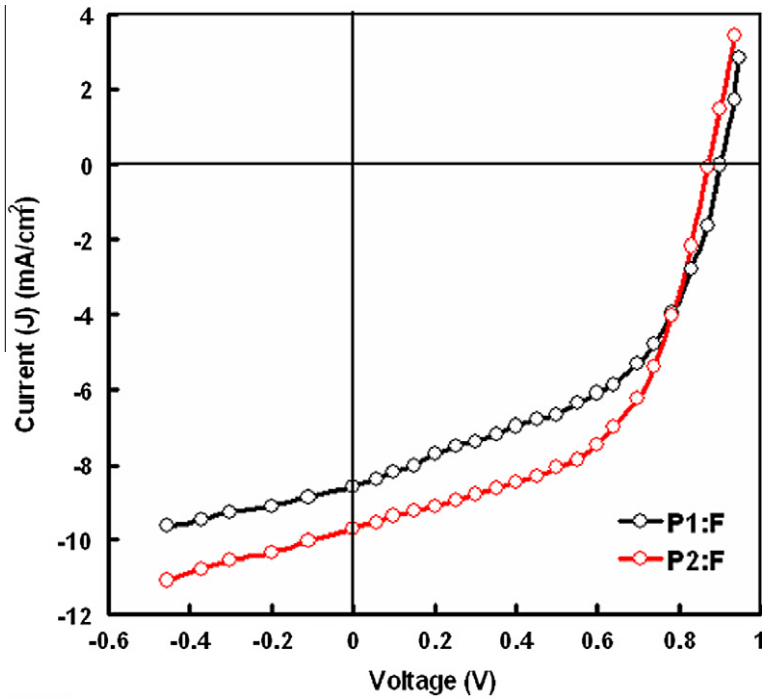

Fig. 5. Current–voltage characteristics, under illumination of the BHJ devices based on solvent annealed **P1**:**F** and **P2**:**F** blends.

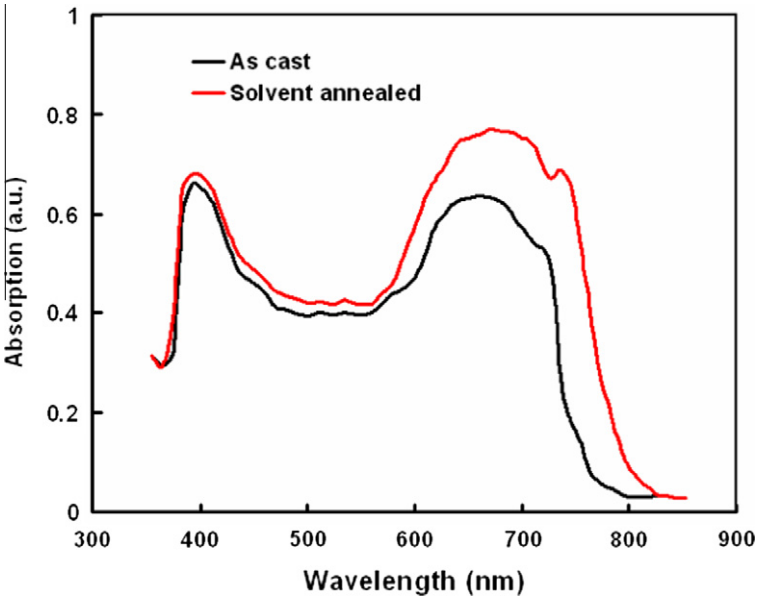

Fig. 6. Normalized optical absorption spectra of the as cast and solvent annealed **P2**:**F** blends.

were estimated from the space charge limited current (SCLC) measurements [25], with hole and electron only devices. Fig. 8 shows the dark current–voltage characteristics of ITO/PEDOT:PSS/**P2**:**F** (as cast or solvent annealed)/Au hole only devices, with corrected bias voltage, which is determined by the work function of Au and HOMO level of the **P2**. Similar results have been observed for devices based on **P1**:**F**. In the higher voltage region, the J–V characteristics can be fitted with SCLC region with trap free limit. The hole mobilities in the blends were estimated by fitting the J–V characteristics with SCLC model (Eq. (2)). The hole mobility in is 2.3×10^{-5} cm^2/Vs and 1.2×10^{-5} cm^2/Vs for as cast and solvent annealed **P2**:**F** blend, respectively. Therefore the hole mobility enhancement upon the solvent annealing is caused by the enhanced π–π^* stacking and chain ordering, as supported by the absorption spectra

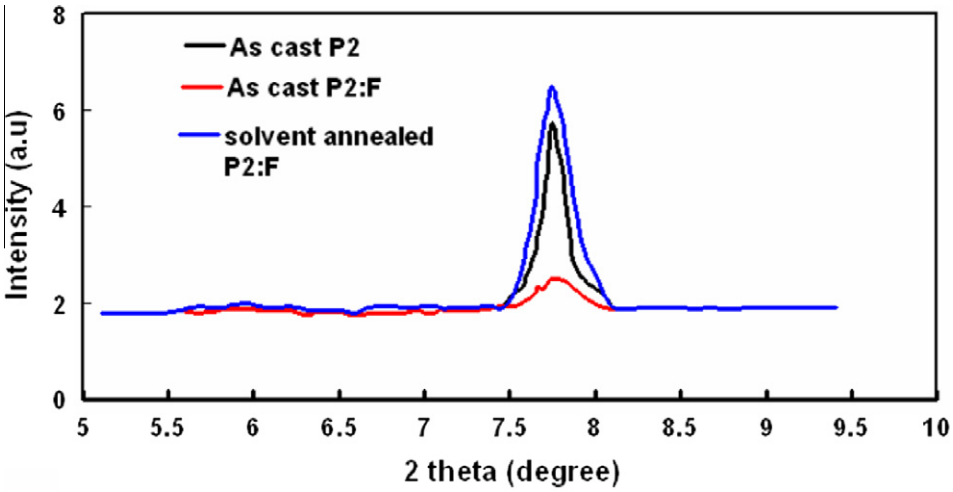

Fig. 7. XRD pattern of as cast **P2**, as cast **P2**:**F** and solvent annealed **P2**:**F** thin films.

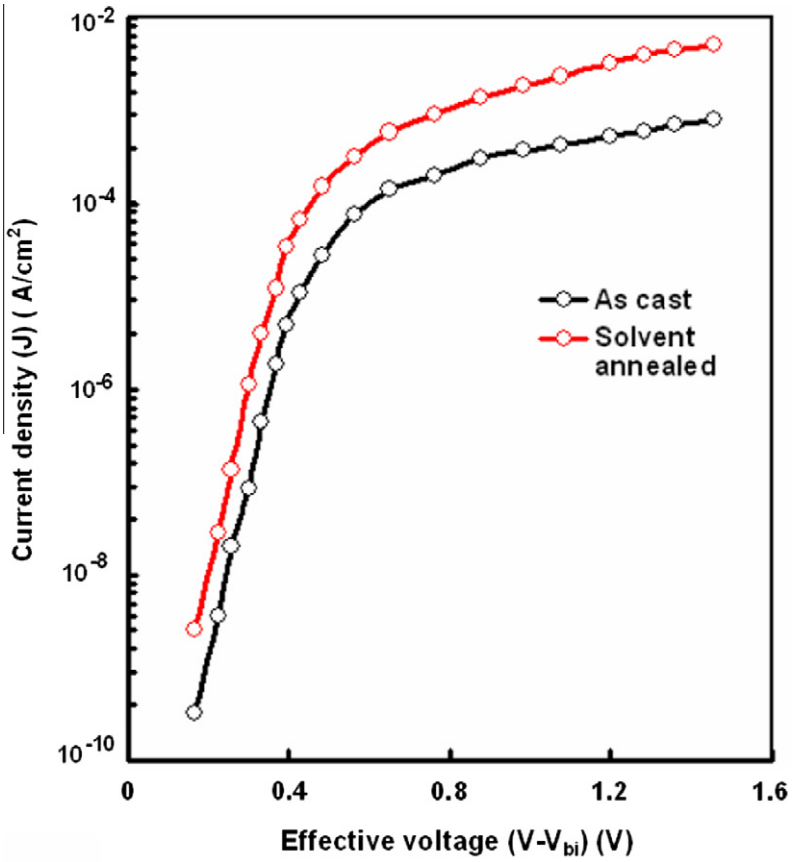

Fig. 8. Current–voltage characteristics in dark for hole only ITO/PEDOT:PSS/**P2**:**F**/Au devices based on as cast and solvent annealed blends.

and XRD pattern. We have also measured the electron mobility in the **P2**:**F** blend for electron only Al/**P2**:**F** (as cast or solvent annealed)/Al device and the electron mobility is 2.4×10^{-4} cm^2/Vs and 3.6×10^{-4} cm^2/Vs for as cast and solvent annealed blends, respectively. The hole mobility increases by about one order of magnitude, but the electron mobility is slightly changed. This observation shows that the **F** domain does not change much with the solvent annealing process. With the hole mobility enhancement and similar value of electron mobility, more balanced electron and hole transport can be achieved, which reduces the formation of space charge, improves

the PCE of the device. The ratio of the electron and hole mobility for the devices based on as cast and solvent annealed blends is 10.4 and 3, respectively. In the case of the device based on as cast blend, the charge transport in unbalanced (hole mobility is much lower than the electron mobility), hole accumulation occurred, near the anode i.e. ITO/PEDOT:PSS electrode and the photocurrent is space charge limited [26]. However, the device processed from the solvent annealed blend, shows the higher value of hole mobility, due to the increased crystalline nature of copolymer, in the blend, whereas, the charge transport in more balanced and the effect of space charge is reduced, resulting improved PCE.

4. Conclusions

The optical and electrochemical properties of two novel low band gap D–A conjugated polymers **P1** and **P2** have been investigated and found that the absorption spectra of these copolymers in thin film form has been extended up to 750 nm and 800 nm for **P1** and **P2**, respectively. The optical band gap of **P1** and **P2** is 1.62 eV and 1.70 eV, respectively. The electrochemical data i.e. HOMO and LUMO energy levels of both **P1** and **P2** indicate that these copolymers are suitable as electron donor with PCBM or modified PCBM **F** as acceptor for efficient BHJ PV devices. The higher value of the V_{oc} for the devices based on **P1** and **P2** with respect to P3HT has been attributed to the deeper HOMO level of both **P1** and **P2** as compared to P3HT. The BHJ PV devices based on the as cast **P1**:PCBM and **P2**:PCBM show an overall PCE about 2.8% and 3.29%, respectively, whereas the PCE values for the devices based on **P1**:**F** and **P2**:**F** exhibit about 3.72% and 4.36%, respectively. The higher values of PCE for the device based on **P2** relative to **P1** is due to the more efficient photo-induced charge transfer and higher value of hole mobility for **P1**. The higher value of devices based on **F** as electron acceptor is ascribed to the higher absorption of coefficient of **F** in visible region as compared to PCBM. We have also investigated the effect of solvent annealing on the photovoltaic response of the BHJ devices based on **P1**:**F** and **P2**:**F** layers and found that the PCE of the devices is about 4.36% and 4.88%, respectively. The increase in the PCE has resulted from the increase in the crystalline nature of copolymer in the blend, which in turn improves the hole mobility. The increase in hole mobility results in a more balanced charge transport in the device.

Acknowledgement

We are thankful to Prof. Y.K. Vijay of Thin film and Membrane Science Laboratory, University of Rajasthan Jaipur (Raj.) for allowing us to undertake the device fabrication and characterization in his laboratory.

References

[1] S.R. Forrest, M.E. Thompson, Chem. Res. 107 (2007) 923.
[2] (a) H. Klauk, A. Wielry (Eds.), Organic electronics: materials, manufacturing and applications, VCH, Weinheim, Germany, 2006;
(b) S. Allard, M. Forster, B. Souharce, H. Theim, U. Scherf, Angew. Chem. Int. Ed. 47 (2008) 4070–4098;
(c) A. Dodabalapur, Mater. Today 9 (2006) 24–30.
[3] (a) H.Y. Chen, J.H. Hou, S.Q. Zhang, Y.Y. Liang, G.W. Yang, Y. Yang, L.P. Yu, Y. Wu, G. Li, Nature Photon 3 (2009) 649;
(b) Y.Y. Liang, Z. Xu, J.B. Xia, S.T. Tsai, Y. Wu, G. Li, C. Ray, L.P. Yu, Adv. Mater. 22 (2010) E135;
(c) J.W. Chen, Y. Cao, Acc. Chem. Res. 42 (2009) 1709;
(d) G. Dennler, M.C. Scharber, C.J. Brabec, Adv. Funct. Mater. 21 (2009) 1323;
(e) Y.J. Chen, S.H. Yang, C.S. Hsu, Chem. Rev. 109 (2009) 5868;
(f) Y.F. Li, Y.P. Zou, Adv. Mater. 20 (2008) 2952;
(g) B.C. Thompson, J.M.J. Frechet, Angew. Chem. Int. Ed. 47 (2008) 58;
(h) F.C. Krebs, Sol. Energy Mater. Sol. Cells 93 (2009) 394.
[4] G. Yu, J. Gao, J.C. Hummelen, F. Wudl, A.J. Heeger, Science, 1995.
[5] (a) I.W. Hwang, Q.H. Zhu, C. Soci, B.Q. Chen, A.K.Y. Jen, D. Moses, A.J. Heeger, Adv. Funct. Mater. 17 (2007) 563;
(b) H. Ohkita, S. Cook, Y. Astuli, W. Duffy, S. Tieney, W. Zang, M. Heeney, I. McCullun, J. Nelson, D.D.C. Bradley, J.R. Durrent, J. Am. Chem. Soc. 130 (2008) 3030;
(c) T. Drori, C.X. Sheng, A. Ndobe, S. Singh, J. Holt, Z.V. Vardeny, Phys. Rev. Lett. 10 (2008) 037401.
[6] (a) G. Li, V. Shrotriya, J. Huang, Y. Yao, T. Moriarty, K. Emery, Y. Yang, Nat. Mater. 4 (2005) 864;
(b) W. Ma, C. Yang, X. Gong, K. Lee, A.J. Heeger, Adv. Funct. Mater. 15 (2005) 1617;
(c) Y. Zhao, Z.Y. Xe, Y. Qu, Y.H. Geng, L.X. Wang, Appl. Phys. Lett. 90 (2007) 043504.
[7] (a) Y.J. He, Y.F. Li, Phys. Chem. Chem. Phys. 13 (2011) 1970;
(b) Y.J. He, Y.H.Y. Chen, J.H. Hou, Y.F. Li, J. Am. Chem. Soc. 132 (2010) 1377;
(c) G.J. Zhao, Y.J. He, Y.F. Li, Adv. Mater. 22 (2010) 4355;
(d) Y.J. He, G.J. Zhao, B. Peng, Y.F. Li, Adv. Funct. Mater. 20 (2010) 3383;
(e) Y.J. Cheng, C.H. Hsieh, Y.J. He, C.H. Hsu, Y.F. Li, J. Am. Chem. Soc. 132 (2010) 17381.
[8] M.C. Scharber, D. Muhlbscher, M. Koppe, P. Denk, C. Waldauf, A.J. Heeger, C.J. Brabec, Adv. Mater. 18 (2006) 789.
[9] (a) J. Roncalli, Chem. Rev. 97 (1997) 173;
(b) E. Zhou, J. Cong, K. Tamija, K. Hashimoto, Chem. Mater. 22 (2011) 4890.
[10] (a) L. Burgi, M. Turbiez, R. Pfeiffer, F. Bienewald, H. Kimer, C. Winnewisser, Adv. Mater. 20 (2008) 2217;
(b) Y. Li, S.P. Singh, P. Sonar, Adv. Mater. 22 (2010) 4862;
(c) H.N. Tsao, D.M. Cho, I. Par, M.R. Hansen, A. Mavrinskiy, D.Y. Yoon, R. Graf, W. Pisula, H. Spiess, K. Mullen, J. Am. Chem. Soc. 133 (2011) 2605.
[11] (a) S.C. Price, A.C. Stuart, W. You, Macromolecules 43 (2010) 4609;
(b) H. Zhou, L. Yang, S.C. Price, K.J. Knight, W. You, Angew. Chem. Int. Ed. 49 (2010) 7992;
(c) B.J.A. Caputo, G.C. Welch, D.A. Kamkar, Z.B. Henson, T.Q. Nguyen, B.C. Bazan, Small 7 (2011) 1422;
(d) P-L.T. Boudreault, A. Najari, M. Leclerc, Chem. Mater. 23 (2011) 456;
(e) G.Y. Chen, Y.H. Cheng, Y.J. Chou, M.S. Su, C.M. Chen, K.H. Wei, Chem. Commun. 47 (2011) 5064;
(f) M. Zhang, X. Guo, Y. Li, Adv. Energy Mater., doi: 10.1002/aenm.201100193.;
(g) Z.G. Zhang, H. Fan, J. Min, S. Zhang, J. Zhang, M. Zhang, X. Guo, X. Zhan, Y. Li, Polym. Chem., doi: 10.1039/C1py00119a.;
(h) Y. Lee, Y.M. Nam, W.H. Lo, J. Mater. Chem. 21 (2011) 8583;
(i) E. Wang, Z. Ma, Z. Zhang, P. Henriksson, O. Inganas, F. Zhnag, M.R. Andersson, Chem. Commun. 47 (2011) 4908;
(j) S. Subramaniyan, H. Xin, F.S. Kim, S. Shoaee, J.R. Durrant, S.A. Jenekhe, Adv. Energy Mater., doi: 10.1002/aenm.201100215.;
(k) Y. Zhang, J. Zou, H.L. Yip, K.S. Chen, J.A. Davies, Y. Sun, A.K.Y. Jen, Macromolecules 44 (2011) 4752;
(l) Q. Shi, H. Fan, Y. Liu, J. Chen, L. Ma, W. Hu, Z. Shuai, Y. Li, X. Zhan, Macromolecules 44 (2011) 4230.
[12] (a) Y. Linag, Z. Xu, J. Xia, S. Tsai, Y. Wu, G. Li, C. Ray, L. Yu, Adv. Mater. 22 (2010) E135;
(b) H.Y. Chen, J. Hou, S. Zhang, Y. Linag, G. Yang, Y. Yang, L. Yu, G. Li, Nature Photon 3 (2009) 649;
(c) S.H. Park, A. Roy, S. Beaupre, S. Cho, N. Coates, J.S. Moon, D. Moses, M. Leclerc, K. Lee, A.J. Heeger, Nature Photon 3 (2009) 297;
(d) C.V. Hoven, X.D. Dang, R.C. Coffin, J. Peet, T.Q. Nguyen, G.C. Bazan, Adv. Mater. 22 (2010) E63;
(e) T.Y. Chu, J. Lu, S. Beaupre, Y. Zhang, J.R. Pouliot, S. Wakim, J. Zhou, M. Leclerc, Z. Li, J. Ding, Y. Tao, J. Am. Chem. Soc. 133 (2011) 4250;
(f) M. Wang, X. Hu, P. Liu, W. Li, X. Gong, F. Huang, Y. Cao, J. Am.

Chem. Soc. 133 (2011) 9638;
(g) S.C. Price, A.C. Stuart, L. Yang, H. Zhou, W. You, J. Am. Chem. Soc. 133 (2011) 4625.
[13] (a) www.solarmer.com.;
(b) www.konarka.com.
[14] (a) J.A. Mikroyannidis, M.M. Stylianakis, P. Balraju, P. Suresh, G.D. Sharma, ACS Appl. Mater. Interfaces 1 (2009) 1711;
(b) J.A. Mikroyannidis, M.M. Stylianakis, P. Suresh, P. Balraju, G.D. Sharma, Org. Electron. 10 (2009) 1320;
(c) J.A. Mikroyannidis, S.S. Sharma, Y.K. Vijay, G.D. Sharma, ACS Appl. Mater. Interfaces 2 (2010) 270;
(d) J.A. Mikroyannidis, A.N. Kabanakis, A. Kumar, S.S. Sharma, Y.K. Vijay, G.D. Sharma, Langmuir 20 (2010) 12909.
[15] (a) J.A. Mikroyannidis, A. Kabanakis, P. Balraju, G.D. Sharma, J. Phys. Chem. C 114 (2010) 12355;
(b) J.A. Mikroyannidis, D.V. Tsagkournos, P. Balraju, G.D. Sharma, Org. Electron. 11 (2010) 1242.
[16] J.A. Mikroyannidis, A.N. Kabanakis, P. Balraju, G.D. Sharma, Macromolecules 43 (2010) 5544.
[17] J.A. Mikroyannidis, A.N. Kabanakis, S.S. Sharma, G.D. Sharma, Adv. Funct. Mater. 21 (2011) 746.
[18] (a) J. Yang, Q. Hou, W. Yang, C. Zhang, Y. Cao, Macromolecules 38 (2005) 244;
(b) C. Kanimozhi, P. Balraju, G.D. Sharma, S. Patil, J. Phys. Chem. B 114 (2010) 3095.
[19] (a) Y.F. Li, Y. Cao, J. Gao, D.L. Wang, G. Yu, A.J. Heeger, Synth. Met. 99 (1999) 243;
(b) Q.J. Sun, H.Q. Wang, C.H. Yang, Y.F. Li, J. Mater. Chem. 13 (2003) 800.
[20] J.H. Hou, M.H. Park, S.Q. Zhang, Y. Yao, L.M. Chen, J.H. Li, Y. Yang, Macromolecules 41 (2008) 6012–6018.
[21] (a) A.P. Zoombelt, M. Fonrodona, M.G.R. Turbiez, M.M. Wienk, R.A.J. Janssen, J. Mater. Chem. 19 (2009) 5336;
(b) E.G. Wang, L.T. Hou, Z.Q. Wang, S. Hellstrom, W. Mammo, F.L. Zhang, O. Inganas, M.R. Andersson, Org. Lett. 12 (2010) 4470.
[22] (a) A.M. Goodman, A. Rose, J. Appl. Phys. 42 (1971) 2823;
(b) D. Chirvase, Z. Chiguvare, M. Knipper, J. Parsis, V. Dyakonov, J.C. Hummelen, Phys. Rev. B 70 (2004) 235207;
(c) H.C.F. Martens, H.B. Brom, P.W.M. Blom, Phys. Rev. B 60 (1999) 8489.
[23] (a) P. Peumans, A. Yakimov, S.R. Forrest, J. Appl. Phys. 93 (2003) 3693;
(b) V.D. Mihailetchi, H. Xie, B. de Boer, L.J.A. Koster, P.W.M. Blom, Adv. Funct. Mater. 16 (2006) 699.
[24] M. Chikamatsu, S. Nagamatsu, Y. Yoshida, K. Satio, K. Yase, Appl. Phys. Lett. 87 (2005) 203504.
[25] (a) M.A. Lampert, P. Mark, Current Injection in Solids, Academic Press, New York, 1970;
(b) V.D. Mihaitetchi, H. Xie, B. de Boer, L.J.A. Koster, P.W.M. Blom, Adv. Funct. Mater. 16 (2006) 699;
(c) Y. Zhao, Z. Xie, Y. Qu, Y. Geng, L. Wang, Appl. Phys. Lett. 90 (2007) 043504.
[26] A.J. Moule, K. Meerholz, Adv. Mater. 20 (2008) 240.